A Novel Wave-Separation Scheme for the Extraction of S-Parameters in Non-TEM Waveguides for the FVTD Method

Dirk Baumann, Christophe Fumeaux, and Rüdiger Vahldieck

Laboratory for Electromagnetic Fields and Microwave Electronics (IFH), ETH Zurich
Gloriastrasse 35, 8092 Zurich, Switzerland, Phone: +41 1 632 5007, Email: dbaumann@ifh.ee.ethz.ch

***Abstract*— This paper proposes an extended scheme for the extraction of scattering parameters for the Finite-Volume Time-Domain (FVTD) method. The flux-splitting algorithm that is inherent to the FVTD method is exploited to compute the incident and reflected fields in a port. A novel correction scheme for the magnetic field is applied that yields accurate results of the scattering parameters in non-TEM structures by performing an artificial flux separation. Multimode S-parameters of a waveguide discontinuity, that are determined using the proposed approach, are successfully validated with a Mode-Matching analysis.**

***Index Terms*— FVTD, scattering parameters, flux splitting.**

I. Introduction

In the Finite-Volume Time-Domain (FVTD) algorithm proposed by Bonnet [1] a flux-splitting scheme is used to perform field updates in the finite-volume mesh cells. For each finite-volume cell outgoing and incoming fluxes are computed through all of its faces. The sum of these fluxes determines the total field variation in the cell. This flux-separation scheme can be exploited for the extraction of scattering parameters, where the outgoing and the incoming fluxes are connected to the incident and the reflected fields [2]. This approach has been successfully applied to TEM structures. Additionally, a mode projection can be used a) in the case of TEM waves to reduce numerical noise and b) in non-TEM guides to extract the generalized scattering matrix.

For non-TEM waves a decrease of the S-parameter's dynamic range has been observed compared to that of TEM waves. This paper first analytically explains the reason for this decrease and then, on this basis, proposes a novel correction scheme, where a frequency-dependent parameter is used to compensate this deficiency. The magnetic field is corrected in order to realize an artificial plane-wave (APW) relationship between the electric $\boldsymbol{E}$ and magnetic field $\boldsymbol{H}^{\text{apw}}$. These corrected fields are used in a flux-splitting scheme to compute the incident and reflected fields for S-parameter extraction.

To demonstrate this wave-separation approach an H-plane rectangular waveguide discontinuity is analyzed. Multi-mode reflection and transmission coefficients of the discontinuity are computed. Results are compared to a Mode-Matching (MM) analysis validating this novel scheme.

II. The FVTD Method

The FVTD method originates from computational fluid dynamics and was adapted for electromagnetics at the end of the 1980s [3]. Maxwell's equations in a conservative form are numerically solved in an unstructured polyhedral (here tetrahedral) mesh. The finite-volume discretization of Maxwell's equations for the tetrahedron i with four triangular faces F_k delimiting the volume V_i can be written as (assuming that the neighboring cell j has the same material)

$$\frac{\partial \boldsymbol{U}_i}{\partial t} = -\frac{1}{V_i}\sum_{k=1}^{4} \boldsymbol{\Phi}_k F_k = -\frac{1}{V_i}\sum_{k=1}^{4}\left(\boldsymbol{\Phi}_{ik}^{+} + \boldsymbol{\Phi}_{jk}^{-}\right) F_k \tag{1}$$

where $\boldsymbol{U} = (E_x, E_y, E_z, H_x, H_y, H_z)^T$ is a vector containing the electric and the magnetic fields. $\boldsymbol{\Phi}_k$ can be interpreted as a flux through the cell face k and can be separated in an incoming $\boldsymbol{\Phi}_{jk}^{-}$ and outgoing $\boldsymbol{\Phi}_{ik}^{+}$ part [1], where only plane waves propagating in direction of the normal vector are considered. Thus, the outgoing flux $\boldsymbol{\Phi}_{ik}^{+}$ out of the cell i is calculated using the field $\boldsymbol{U}_i$ in this cell, and the incoming flux $\boldsymbol{\Phi}_{jk}^{-}$ is computed on the basis of the field $\boldsymbol{U}_j$ in the neighboring cell j

$$\boldsymbol{\Phi}_{ik}^{+} = \boldsymbol{F}(\boldsymbol{n}_k)_i^{+} \cdot \boldsymbol{U}_{ik}^{*} \tag{2}$$

$$\boldsymbol{\Phi}_{jk}^{-} = \boldsymbol{F}(\boldsymbol{n}_k)_j^{-} \cdot \boldsymbol{U}_{jk}^{*} \tag{3}$$

where $\boldsymbol{n}_k = (n_{kx}, n_{ky}, n_{kz})^T$ is the outwards-pointing normal vector of the face k. The matrix $\boldsymbol{F}(\boldsymbol{n}_k)_i^{+}$ is given in equation (5), where c_i is the velocity of light in the medium and following abbreviations are used

$$a_1 = n_{kx}^2 + n_{ky}^2 \quad a_2 = n_{kx}^2 + n_{kz}^2 \quad a_3 = n_{ky}^2 + n_{kz}^2$$
$$a_4 = n_{kx}n_{ky} \quad a_5 = n_{kx}n_{kz} \quad a_6 = n_{ky}n_{kz}$$

The matrix for the incoming flux is related to (5) by

$$\boldsymbol{F}(\boldsymbol{n}_k)_i^{-} = -\boldsymbol{F}(-\boldsymbol{n}_k)_i^{+} \tag{4}$$

In equations (2) and (3) the asterisk in $\boldsymbol{U}_k^{*}$ denotes field values on the triangular face. These fields can be, in a first-order approximation, set equal to the ones in the cell's barycenter. As a second-order approximation the monotonic upwind scheme for conservation laws (MUSCL) can be applied [1].

$$
\boldsymbol{F}(\boldsymbol{n}_k)_i^{+} = \begin{pmatrix} \boldsymbol{F}(\boldsymbol{n}_k)_{i,x}^{H+} \\ \boldsymbol{F}(\boldsymbol{n}_k)_{i,y}^{H+} \\ \boldsymbol{F}(\boldsymbol{n}_k)_{i,z}^{H+} \\ \boldsymbol{F}(\boldsymbol{n}_k)_{i,x}^{E+} \\ \boldsymbol{F}(\boldsymbol{n}_k)_{i,y}^{E+} \\ \boldsymbol{F}(\boldsymbol{n}_k)_{i,z}^{E+} \end{pmatrix} = \frac{1}{2} \begin{pmatrix} a_3 c_i & -a_4 c_i & -a_5 c_i & 0 & n_{kz}/\varepsilon_i & -n_{ky}/\varepsilon_i \\ -a_4 c_i & a_2 c_i & -a_6 c_i & -n_{kz}/\varepsilon_i & 0 & n_{kx}/\varepsilon_i \\ -a_5 c_i & -a_6 c_i & a_1 c_i & n_{ky}/\varepsilon_i & -n_{kx}/\varepsilon_i & 0 \\ 0 & -n_{kz}/\mu_i & n_{ky}/\mu_i & a_3 c_i & -a_4 c_i & -a_5 c_i \\ n_{kz}/\mu_i & 0 & -n_{kx}/\mu_i & -a_4 c_i & a_2 c_i & -a_6 c_i \\ -n_{ky}/\mu_i & n_{kx}/\mu_i & 0 & -a_5 c_i & -a_6 c_i & a_1 c_i \end{pmatrix} \tag{5}
$$

III. S-Parameter Extraction

A method for calculating the generalized scattering matrix using the FVTD method is proposed in [2]. To validate this approach, the reflection coefficient of a coaxially-fed balun was computed and very good agreement to measurements was found. The separated fluxes were used to find the tangential electric field in a port plane

$$
\boldsymbol{E}_t^{+/-} = -\boldsymbol{n}_k \times \mu \boldsymbol{\Phi}_k^{E+/-} \tag{6}
$$

For TEM waves this approach has worked accurately. In non-TEM situations, however, it has been found that the proposed method shows a decrease of the S-parameter's dynamic range.

In this paper the approach of flux separation for determining the incident a and reflected b waves in a waveguide, as proposed in [2], is extended in order to increase the dynamic range of the extraction scheme in non-TEM cases. In this section an artificial flux-separation scheme is proposed, that enhances the original flux-separation for the extraction of generalized scattering parameters. This correction scheme makes use of frequency-dependent parameters. Frequency-domain (FD) values are retrieved from time-domain values by a Discrete Fourier Transform performed on the fly during the FVTD iteration. In the following FD terms are denoted with a hat $\breve{}$.

A. TEM Waves

Assume a plane wave with components E_y and H_x travelling in positive z-direction. If the flux separation is performed on a port plane that is perpendicular to the propagation direction $\boldsymbol{n} = (0,0,1)^T$, the outgoing $(+)$ and the incoming $(-)$ flux for the electric field can be written in a simplified form

$$
\breve{\Phi}_x^{E^+} = \frac{1}{2}\left(-\frac{1}{\mu}\breve{E}_y + c\breve{H}_x\right) = -\frac{1}{2\mu}\left(\breve{E}_y - Z_\mathrm{w}\breve{H}_x\right) \tag{7}
$$

$$
\breve{\Phi}_x^{E^-} = \frac{1}{2}\left(-\frac{1}{\mu}\breve{E}_y - c\breve{H}_x\right) = -\frac{1}{2\mu}\left(\breve{E}_y + Z_\mathrm{w}\breve{H}_x\right) \tag{8}
$$

Here, the outgoing flux $\breve{\Phi}_x^{E+}$ is associated to the incident field a and the incoming flux $\breve{\Phi}_x^{E-}$ to the reflected field b. In the case of a plane wave propagating only in $+z$-direction, there is no reflected field and thus the incoming flux $\breve{\Phi}_x^{E-}$ must be zero. This can be proved, if using the relation between the electric and magnetic field of a plane wave $\breve{E}_y/\breve{H}_x = -Z_\mathrm{w}$ and inserting it in equation (8).

B. Non-TEM Waves

In non-TEM guides the incoming flux (8) is not equal to zero, even if there is no reflected wave. In the following it will be shown that this condition can be re-established with an appropriate correction factor.

In a rectangular waveguide the relation between the electric and the magnetic field in the case of a TE-mode can be written as

$$
\frac{\breve{E}_y}{\breve{H}_x} = -Z_\mathrm{TE} \tag{9}
$$

Obviously, using relation (9) the incoming flux (8) does not become zero. Moreover, the reflection coefficient, computed as the ratio of incoming and outgoing flux, yields

$$
S_{11} = \frac{Z_\mathrm{TE} - Z_\mathrm{w}}{Z_\mathrm{TE} + Z_\mathrm{w}} \tag{10}
$$

Figure 1 shows the analytical result of (10) in comparison to the ratio of the simulated incoming to outgoing fluxes in a WR28 waveguide. Hence, the S-parameter extraction scheme is limited in the non-TEM case by the waveguide's geometry, the considered modes and the operational frequency.

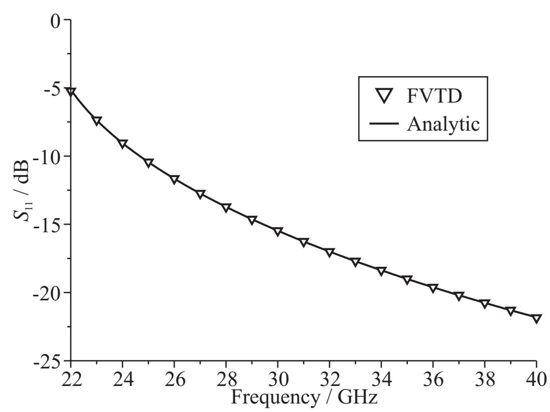

Fig. 1. Comparison between analytical and numerical result of the ratio of the outgoing and the incoming fluxes in a port.

C. Correction Scheme

In order to ensure correct results from the flux-splitting S-parameter extraction scheme, the electric and magnetic fields must be forced to yield a plane wave. For a TE mode with cut-off frequency f_c, the magnetic field can be expressed as

$$\breve{H}_x = -\frac{\breve{E}_y}{Z_\mathrm{w}}\sqrt{1-\left(\frac{f_c}{f}\right)^2} \tag{11}$$

If the magnetic field is multiplied with a correction factor, an artificial plane wave (APW) can be created

$$\breve{H}_x^\mathrm{apw} = \frac{\breve{H}_x}{\sqrt{1-\left(\frac{f_c}{f}\right)^2}} = C_\mathrm{apw}^\mathrm{TE}\cdot\breve{H}_x \tag{12}$$

The frequency and geometry dependent correction factor $C_\mathrm{apw}^\mathrm{TE}$ can be calculated from the mode-template vector, see section III-D. For TM modes a correction factor can be found correspondingly.

The relation between the electric and the magnetic field of the APW thus becomes

$$\frac{\breve{E}_y}{\breve{H}_x^\mathrm{apw}} = -Z_\mathrm{w} \tag{13}$$

The magnetic field (12) is used in equations (7) and (8) yielding an artificial flux splitting, which is used exclusively to extract S-parameters. The regular field update of the tetrahedra remains unaffected.

In the case of a TE wave propagating in positive z-direction, having an incident (i) and reflected (r) component, the fluxes become

$$\breve{\Phi}_x^{E+} = -\frac{1}{\mu}\breve{E}_y^i \tag{14}$$

$$\breve{\Phi}_x^{E-} = -\frac{1}{\mu}\breve{E}_y^r \tag{15}$$

It can be shown that introducing H_x^apw does not only yield correct fluxes, but additionally results in the correct power in a port. The power density of a TE wave is connected to the artificial fluxes according to

$$\breve{S} = \frac{1}{2}\frac{|\breve{E}_y|^2}{Z_\mathrm{TE}} = \frac{1}{2}\frac{|\breve{\Phi}_x^E|}{Z_\mathrm{TE}}\mu^2\,. \tag{16}$$

D. Mode Projection

In a multi-mode environment, each electromagnetic mode on a physical port is assigned to one electromagnetic port p. To separate the fields of a certain mode, its mode-template vector $\boldsymbol{e}_p$ ([4], [5]) has to be known a-priori, either analytically or from an eigenmode analysis. The mode projection yields the mode amplitude in the port p consisting of K triangles

$$\breve{A}_p^{+/-} = \sum_{k=1}^{K}\breve{\boldsymbol{E}}_t^{+/-}(k)\cdot\boldsymbol{e}_p(k)F_k \tag{17}$$

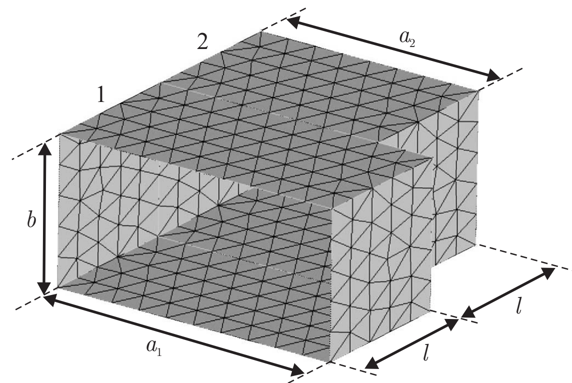

Fig. 2. Geometry of the H-plane step discontinuity. Only the triangular surface mesh is shown.

where the tangential field $\breve{\boldsymbol{E}}_t^{+/-}$ is determined using (6), and (7)-(8) with the corrected H-field (12). The incident and the reflected wave can now be computed with

$$a_p = \frac{\breve{A}_p^+}{\sqrt{Z_{\mathrm{TE_p}}}} \tag{18}$$

$$b_p = \frac{\breve{A}_p^-}{\sqrt{Z_{\mathrm{TE_p}}}} \tag{19}$$

As validation, in chapter IV the extraction of the scattering parameters of a waveguide discontinuity is shown and compared to a reference solution.

IV. H-Plane Step Discontinuity

The flux-splitting procedure is used to compute the scattering parameters of a rectangular waveguide H-plane step discontinuity. A MM analysis is serving as a reference solution.

The geometry including the meshed surface is depicted in Fig. 2. The feeding guide 1 is a WR75 waveguide with the dimensions $a_1 = 19.05\,\mathrm{mm}$ and $b = 9.525\,\mathrm{mm}$. The subsequent waveguide 2 has the width $a_2 = 15.2\,\mathrm{mm}$ and the same height b. The port planes are located at the same distance from the discontinuity ($l = 1.5\,\mathrm{mm}$). A Gaussian pulse that covers the necessary bandwidth is used for exciting the fundamental TE_{10} mode. The reflection coefficient $S_{11}(1,1)$ for the fundamental mode is shown in Fig. 3. The solid line displays the MM analysis, and the triangles the result obtained from the FVTD analysis. A good agreement is achieved over the whole frequency range. The transmission coefficient $S_{21}(1,1)$ for the fundamental mode is plotted in Fig. 4. The result shows, that the use of the flux-splitting scheme yields the correct power in a port plane as explained in section III-C. Using the mode projection, the generalized scattering matrix can be obtained. Figure 5 depicts the reflection coefficient $S_{11}(2,1)$ from the incident fundamental mode

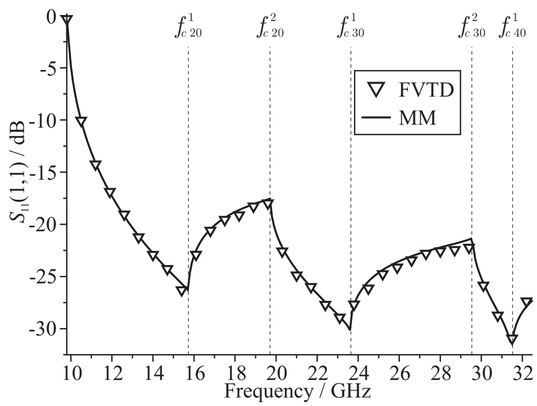

Fig. 3. Comparison between FVTD and MM results of the reflection coefficient $S_{11}(1,1)$ for the fundamental mode at the H-Plane step discontinuity.

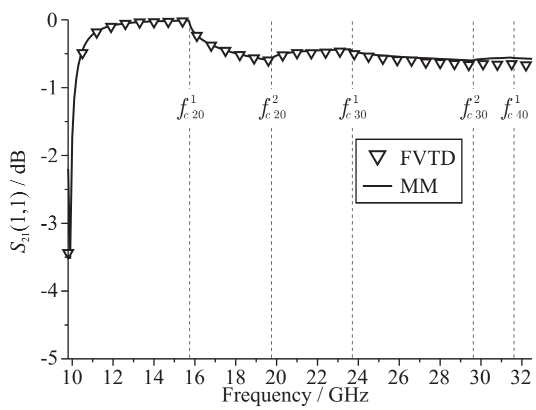

Fig. 4. Comparison between FVTD and MM results of the transmission coefficient $S_{21}(1,1)$ for the fundamental mode at the H-Plane step discontinuity.

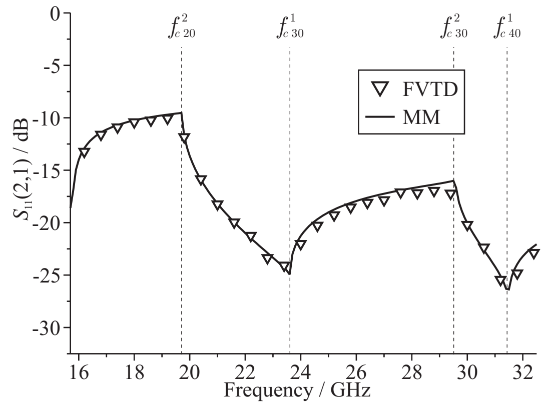

Fig. 5. Comparison between FVTD and MM results of the reflection coefficient $S_{11}(2,1)$ from incident TE_{10} into reflected TE_{20} mode at the H-Plane step discontinuity.

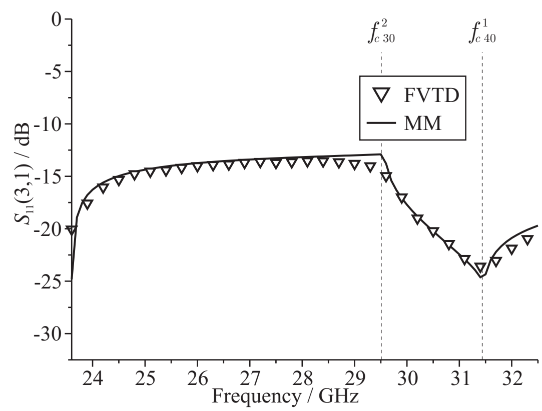

Fig. 6. Comparison between FVTD and results of the reflection coefficient $S_{11}(3,1)$ from incident TE_{10} into reflected TE_{30} mode at the H-Plane step discontinuity.

to the reflected TE_{20} mode. Again, the agreement between the FVTD result and the MM analysis is good. Also the reflection from the incident TE_{10} to the TE_{30} mode shows a good agreement, as can be seen in Fig. 6. The slight offset of the FVTD results compared to the MM result for $f > 30$ GHz is due to the, for high frequencies, coarse mesh discretization in the waveguide.

V. Conclusion

An improved scheme for the use of the FVTD's flux separation algorithm to extract generalized S-parameters for non-TEM waveguides is proposed in this paper. The magnetic field is properly adjusted by a correction factor in order to achieve an artificial plane-wave relationship between the electric and the magnetic field. Thus, the extended flux-splitting algorithm yields correct and accurate results for the computation of the incident and the reflected waves in a port. The novel scheme is validated by comparing the results from a FVTD analysis of the S-parameter of a waveguide discontinuity to those obtained from a MM analysis. Although the proposed scheme is intended and tested for FVTD, it is believed that it can be used in other numerical time-domain techniques.

References

[1] P. Bonnet, X. Ferrieres, B. Michielsen, and P. Klotz, *Time Domain Electromagnetics*. S. M. Rao, Ed., Academic Press, 1997, ch. 9, pp. 307–367.

[2] D. Baumann, C. Fumeaux, P. Leuchtmann, and R. Vahldieck, "Generalized-scattering-matrix extraction using the finite-volume time-domain (FVTD) method," in *IEEE MTT-S Int. Microwave Symp. Dig.*, Fort Worth, TX, June 2004, pp. 1701–1704.

[3] V. Shankar, A. H. Mohammadian, and W. F. Hall, "A time-domain, finite-volume treatment for the maxwell equations," *Electromagnetics*, vol. 10, pp. 127–145, 1990.

[4] E. A. Navarro, T. M. Bordallo, and J. Navasquillo-Miralles, "FDTD characterization of evanescent modes - multimode analysis of waveguide discontinuities," *IEEE Trans. Microwave Theory Tech.*, vol. 48, no. 4, pp. 606–610, 2000.

[5] W. K. Gwarek and M. Celuch-Marcysiak, "Wide-band S-parameter extraction from FD-TD simulations for propagating and evanescent modes in inhomogeneous guides," *IEEE Trans. Microwave Theory Tech.*, vol. 51, no. 8, pp. 1920–1928, 2003.